

EVIDENCE OF VOIDS WITHIN THE AS-DEPOSITED STRUCTURE OF GLASSY SILICON

S. C. Moss and J. F. Graczyk

Department of Metallurgy and Materials Science, Massachusetts Institute of Technology,
Cambridge, Massachusetts 02139

(Received 8 October 1969)

We present electron diffraction data from amorphous silicon which cannot be reconciled with the intensity profiles derived from small-crystallite models based on the diamond structure. Our diffraction patterns do reveal a pronounced low-angle scattering which anneals out on progressive heating and is indicative of actual void spaces, or regions of distinctly deficient density, in the films. These regions may be responsible for the recent observations of Brodsky and Title on surface states within the bulk of amorphous Si.

We are currently preparing for publication an extensive electron diffraction study of the structure and mode of crystallization of amorphous silicon. In the course of this work we have naturally considered various models by which to characterize the short-range structure and we would like to report here some of our conclusions. Several workers have noted the inappropriateness of a model for amorphous Si or Ge which is based solely on the positions and coordinations found in the diamond structure. Coleman and Thomas,¹ Grigorovici,² and more recently Grigorovici and Manaila³ suggest that the structure may be an appropriate mixture of configurations found in the diamond-cubic and pentagonal-dodecahedral arrangements (the staggered and eclipsed configurations³). They present³ a fit to the radial density function (RDF) of Richter and Breitling⁴ for amorphous Ge whereby some measure of success is achieved. The model, however, appears a bit artificial and cannot be described as unique; but it is unfortunately true with amorphous solids that, far from having a surfeit of good fits to models, one usually cannot find any model which gives a passable fit. This situation is summarized by Cargill⁵ for the amorphous phase of alloys with the close-packed structure, for which only the calculations of Dixmier, Doi, and Guinier⁶ seem to provide any agreement with experiment.⁷

For the present we would like to compare the electron-diffraction pattern of amorphous silicon with models based on distributions of small crystals with diamond structure. The data were collected using a scanning diffraction instrument with energy filtering of the diffracted electrons.⁸ The measured intensity has been normalized to the independent scattering curve for silicon at high s , where $s = 4\pi \sin\theta/\lambda$, and has thereby been put into the appropriate absolute units. All experimental details including the data handling and analysis will be discussed elsewhere. In Fig.

1(d) is plotted the result for a 100-Å Si film vapor-deposited onto NaCl and removed from the substrate to a 75-mesh grid for diffraction. $F(s)$

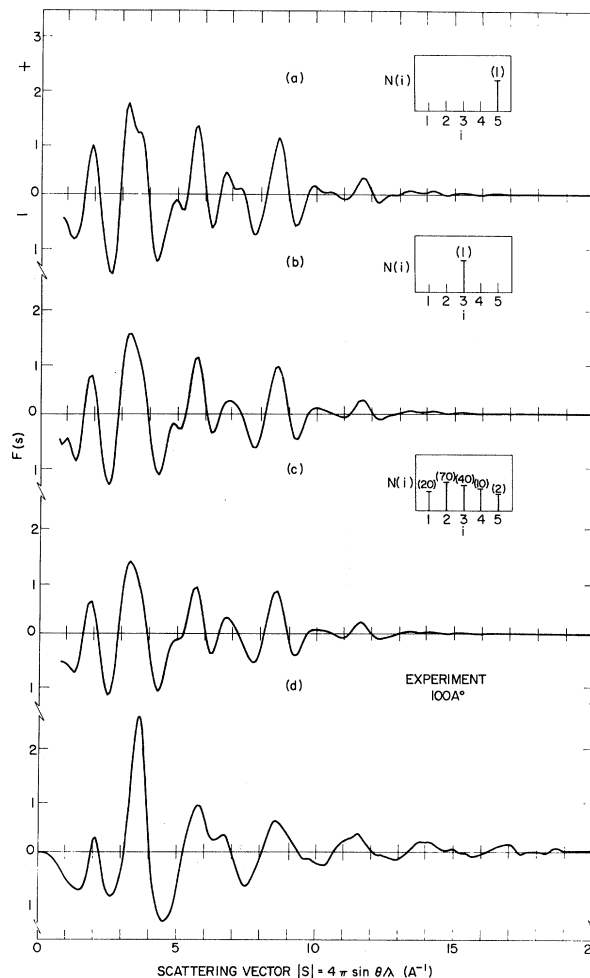


FIG. 1. The reduced intensity function $F(s)$. (a)-(c) Various diamond-cubic microcrystallite calculations: (a), for five neighbor coordination shells about a central origin (47 atoms); (b), for three neighbor shells (29 atoms); (c), for the crystallite distribution shown in the insert. (d) Experiment on a 100-Å amorphous Si film.

is a reduced intensity function given by

$$F(s) = s(I/ff^* - 1) = \int_0^\infty 4\pi r[\rho(r) - \rho_0] \sin(sr) dr.$$

I is the normalized intensity, ff^* is the product of the atomic scattering factor and its complex conjugate, $\rho(r)dr$ is the number of atoms in a spherical shell between r and $r+dr$, and ρ_0 is the average atomic density. Figures 1(a)-1(c) are attempts to match the data in 1(d) with various microcrystalline distributions. $F(s)$ for any crystallite is simply calculated using the Debye intensity function where

$$F(s) = \frac{1}{N} \sum_{m \neq n} [\sin(sr_{mn})/r_{mn}] \exp(-2M_{mn}),$$

and the sum is carried out for all atom pairs in a

crystallite containing N atoms. The function $\exp(-2M_{mn})$ was actually taken outside the summation and made equal to the Debye-Waller factor for silicon. Since nearest neighbors (especially in tetrahedrally bonded silicon) will not vibrate against each other as much as the independent relative displacement of distant neighbors, the use of an average $2M$ will overdamp somewhat the calculated curves. Such calculations have already been performed for crystalline diamond⁹ (without a temperature factor), but they were for larger sizes and did not include any crystallite distributions.

It should be pointed out that when amorphous Si crystallizes the first diffuse peak in $F(s)$ is converted into the (111) reflection while the next two Bragg peaks, (220) and (311), as in Fig. 2(b),

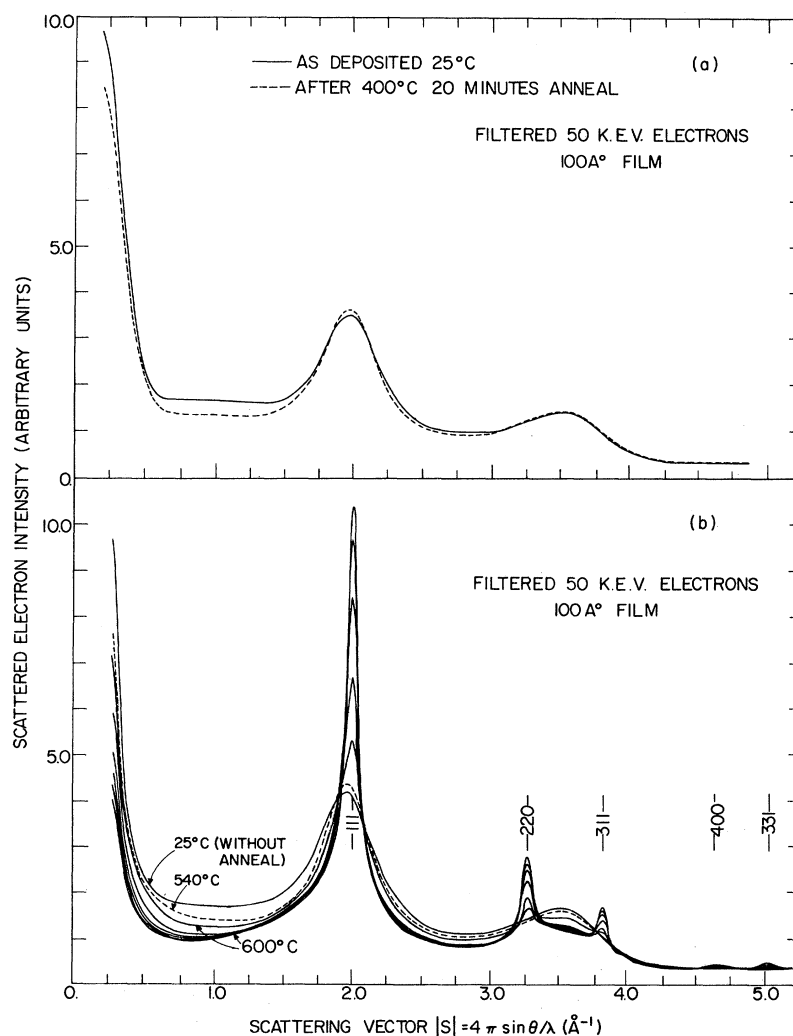


FIG. 2. (a) Experimental intensity profiles at room temperature from a 100- \AA amorphous Si film as deposited and after a 20-min anneal at 400°C; (b) a series of diffraction profiles run at temperature, as a function of increasing temperature up to 600°C, and then as a function of time at 600°C. The two traces in (a) and the several in (b) each took about 40 sec to complete.

grow out of the second diffuse peak. Therefore the sharpness and symmetry, especially of the second peak in the experimental $F(s)$, provide strong evidence against a crystallite interpretation. In Fig. 1, $N(i)$ is the number of crystallites in the distribution having atoms out to the i th coordination shell. If $i=1$ we have just a central atom and its four first neighbors. If $i=2$ we have first- and second-neighbor shells in the crystallite—a total of 17 atoms. If $i=3$ we have 29 atoms, and so forth. We should emphasize that we are here calculating the intensity for symmetrical spherical particles of the diamond cubic structure and are not including correlations between particles because to do so would imply an even larger range crystallinity. If these results disagree badly with experiment, then we would be forced to conclude that the films should not be characterized by a distribution of crystallites of these sizes.

Figure 1(a) is the largest crystallite considered, extending to five neighbors, which represents a spherical particle with 47 atoms and a diameter equal to about 12 Å. We stopped there because we observed appreciable nonrandom correlations in our transform of $F(s)$ [in $4\pi r\{\rho(r) - \rho_0\}$] only out to about 10–11 Å. Figure 1(a) thereby demonstrates the pattern from the largest crystallite we should have, if we had them. The peak splitting (220)-(311) is apparent. In order to remove the peak splitting and asymmetry, we have to peel off atoms down to the third-nearest-neighbor shell—a 9-Å-diam particle. Here, in Fig. 1(b), we have a first diffuse peak at about $s=1.95$, whereas the same peak in the experimental curve is less intense and comes at ~ 2.05 . This is a reversal of the order of peak positions for the amorphous and crystalline phases [see Fig. 2(b)]. It is a consequence both of the small crystallite size⁹ and of the fact that, because the first amorphous peak is broad, multiplication of $I(s)$ by s shifts this peak in $F(s)$ to larger values. As the crystallite size increases, the calculated first peak moves to its “proper” position at $s=2.005$ and in an $I(s)$ plot, the order observed in Fig. 2(b) is recovered. The second peak in the model curve is twice as broad and half as intense as in the experiment, and is shifted from $s \approx 3.63$ down to $s \approx 3.44$. The third model peak occurs at ~ 4.91 where the data show nearly a minimum. And so we may proceed to demonstrate that for a particle small enough to give no (220)-(311) splitting, the agreement with experiment is not good.

Another reason that the disagreement for this particle is compelling is that it ($i=3$) represents the smallest crystallite that can distinguish between the diamond-cubic and pentagonal-dodecahedral arrangements. Both models put nearly perfect tetrahedra together but only the diamond cubic gives a peak near the third-nearest-neighbor distance in the experimental RDF (ours and that of Ref. 1).

We display the distribution in Fig. 1(c) for completeness [$F(s)$ is here an appropriately weighted sum over the crystallites] because if we have correlations out to nearly 12 Å then we must include at least a few particles of that diameter. These larger-range correlations are weighted down by the distribution, and the fit in this case, as in the large number of others we tried, is no better.

It might be argued that for such small particles there are surface relaxation effects and homogeneous strains, so that the crystalline spacings would be different from the bulk values. Perhaps so, but in our Fourier transform of $F(s)$ we observe a well-defined tetrahedral arrangement of nearest neighbors at a distance given exactly by the crystal spacing of 2.35 Å and characterized by a breadth in the RDF that can nearly be accounted for solely by thermal vibrations.

If the microcrystallite model is not terribly useful—does not fit the data—then we must look for another interpretation of the spin-resonance results of Brodsky and Title.¹⁰ To this end we have included Fig. 2 which demonstrates the appreciable low-angle scattering that we have invariably observed in our diffraction patterns. Well below the first diffuse peak, the measured intensity should extrapolate smoothly to a small value at $s=0$, instead of which, in our as-deposited samples, it levels off and then rises. Of course it must rise once we are into the main transmitted beam, but in Fig. 2, off the most steeply rising portion, we are at worst at the very tail of the direct beam and are really observing structural effects.

Since a film made up of densely packed particles, either crystallites or glassy material of near-crystalline density, cannot give such low-angle scattering,¹¹ we are forced to conclude that it arises from the presence of voids or pores—regions of appreciable density deficiency within the films. These regions, however, are not so distinct as to be observable under high-resolution electron microscopy. The scattering is not due to contamination because films held in the instru-

ment at room temperature for up to $\frac{1}{2}$ h show no changes in scattering at low angles, and it is not a substrate effect. If we include the low-angle part of the intensity when we Fourier transform the data, the ρ_0 estimated from the small r region of the transform is around 10-15% lower than the crystalline density. If we cut out the low-angle data and extrapolate the intensity smoothly down to a small value at $s=0$, we get values close to the crystalline density. This is as it should be since the distribution of low-density material in this case affects mainly the low-angle scattering, and a determination of ρ_0 which neglects the intensity at small s will not notice the pores. This perhaps sheds some light on the variation in density reported, for example, for amorphous Ge.^{12,13} Depending upon how the films are made (deposition rate, etc.) Mogab¹⁴ has carefully measured density deficiencies of from 5 to 25% in $\sim 1\text{-}\mu$ amorphous Si. Presumably the tendency to form voids persists even in these thicker films.

The effects of heating are shown in Fig. 2. Initially we might expect the pores to anneal out on heating without much else occurring by way of structural reorganization. Certainly after crystallization they should disappear and the low-angle scattering should decrease significantly. In Fig. 2(a) we show two direct intensity traces one of which is from as-deposited Si at room temperature and the other, the same 100-Å film heated to 400°C for 20 min and cooled to room temperature—all within the diffraction chamber. In the second trace we can see a noticeable decrease in low-angle scattering, especially at the lowest angles, and the leveling off at $s \approx 1.0$ has diminished. We also almost always see, in these films annealed below crystallization, a small sharpening of the first diffuse peak; but it is not shifted toward the (111) position and there is no change in the second diffuse peak. In Fig. 2(b) we see successive traces as a film is heated up to and through its crystallization temperature (in this case around 580°C—it varies a bit from film to film). The crystallization is obviously heterogeneous because Bragg peaks of the crystalline phase begin to appear on top of, in conjunction with, the amorphous background. [Notice also the shifting of the (111) intensity to a higher s value.] As the transformation proceeds the low-angle intensity progressively falls off signifying finally the annealing out of the void spaces.

These observations can be related to the strik-

ing results of Brodsky and Title on surface defects, within as-deposited films, which anneal out on heating (this does not necessarily require the pores annealing out—just the surface states). Together they strongly suggest that the precrystallization annealing behavior observed in various property measurements may be due to the presence of the postulated free volume. If the defects are indeed the “dangling bonds” usually associated with crystal surfaces then, because amorphous Si has a rather well-defined tetrahedral coordination, the amorphous surface should afford a similar environment. While granting that our films are very thin and may have defects peculiar to their size, we find such an interpretation of the thick-film results tempting, and it would be worthwhile to perform selected low-angle x-ray experiments on some thicker films. In any case, it would seem unlikely that amorphous silicon can be characterized by microcrystallites that have atomic arrangements like the diamond-cubic bulk crystal.

It is a pleasure to thank C. J. Mogab for preparing our films and for several interesting discussions both of our results and his. We would also like to thank Derek Dove, who is currently studying amorphous Ge and finding effects similar to those reported here, for some illuminating remarks—especially on the influence of the low-angle scattering on the density determination.

This research was sponsored by the Advanced Research Projects Agency through the Center for Materials Science and Engineering at Massachusetts Institute of Technology, and we gratefully acknowledge their continued support.

¹M. V. Coleman and D. J. D. Thomas, *Phys. Status Solidi* **24**, K11 (1967).

²R. Grigorovici, *Mat. Res. Bull.* **3**, 13 (1968).

³R. Grigorovici and R. Manaila, to be published.

⁴H. Richter and G. Breitling, *Z. Naturforsch.* **13a**, 988 (1958).

⁵G. S. Cargill, III, to be published.

⁶J. Dixmier, K. Doi, and A. Guinier, in *Physics of Noncrystalline Solids*, edited by J. A. Prins (North-Holland Publishing Company, Amsterdam, The Netherlands, 1965).

⁷Most recently Cargill has applied some calculations of J. L. Finney on the dense random packing of hard spheres to amorphous Ni-P alloys and obtained very interesting coincidences in the second-neighbor peak splitting in the RDF: G. S. Cargill, III, to be published.

⁸J. F. Graczyk and S. C. Moss, *Rev. Sci. Instr.* **40**, 424 (1969).

⁹V. H. Tiensuu, S. Ergun, and L. E. Alexander, J. Appl. Phys. **35**, 1718 (1964).

¹⁰M. H. Brodsky and R. S. Title, Phys. Rev. Letters **23**, 581 (1969).

¹¹A. Bienenstock and B. G. Bagley, J. Appl. Phys. **37**,

4840 (1966).

¹²T. B. Light, Phys. Rev. Letters **22**, 999 (1969).

¹³T. M. Donovan, W. E. Spicer, and J. M. Bennett, Phys. Rev. Letters **22**, 1058 (1969).

¹⁴C. J. Mogab, private communication.

MAGNETIC CLUSTERS ASSOCIATED WITH ISOLATED Fe ATOMS IN PARAMAGNETIC Cu-Ni ALLOYS*

L. H. Bennett and L. J. Swartzendruber

Institute for Materials Research, National Bureau of Standards, Gaithersburg, Maryland 20760

and

R. E. Watson†

Brookhaven National Laboratory,‡ Upton, New York 11973

(Received 23 September 1969)

A small magnetic cluster is shown to exist around an isolated Fe atom in $\text{Cu}_{1-x}\text{Ni}_x$ alloys with a magnetic moment and saturation hyperfine field depending on the number n of Ni near neighbors. This small cluster changes abruptly from moments of $(2.85 + 0.6n) \times \mu_B$ to large moments $[(\sim 17 \text{ to } 20)\mu_B]$ for Ni concentrations near the critical composition. The moment compensation (Kondo effect) found for isolated Fe in Cu appears to persist in Cu-Ni up to at least 10 at.% Ni.

Giant moment clusters ($\sim 10\mu_B$) with large spatial extent have been reported¹⁻⁴ in the critical region ($0.4 \leq x \leq 0.5$) bounding the ferromagnetic Ni-rich $\text{Cu}_{1-x}\text{Ni}_x$ alloys. In the present Letter we report Mössbauer-effect results for isolated Fe atoms (i.e., sources) in both the Cu-rich ($x \leq 0.33$) and in the critical region of Cu-Ni alloys. In the critical region the presence of an Fe atom nucleates a giant moment of $17\text{--}20\mu_B$. In the non-ferromagnetic Cu-rich alloys, the data are readily understood in terms of a distinctly different small cluster confined largely to the Fe atom and the nearest-neighbor shell of surrounding atoms. We find that a simple model of the cluster, with near-neighbor Cu atoms magnetically inert and Ni atoms active,⁵ predicts the complex Mössbauer spectra observed at compositions of $x = 0.1, 0.21, \text{ and } 0.33$. The data also suggest that the Kondo effect is present in the $x = 0.1$ alloys, with a Kondo temperature T_K of ~ 3 K. This is to be compared with $T_K \sim 16$ K (as defined from Mössbauer data) for Fe in pure Cu.^{6,7}

Any investigation of the $\text{Cu}_{1-x}\text{Ni}_x$ system raises the obvious question of atomic clustering. The small amount of short-range order found⁸⁻¹⁰ in slow-cooled alloys with x near 0.5 would not substantially alter our conclusions. Our alloys were rapidly quenched from high temperature, with correspondingly less clustering.¹¹

Our "small"-cluster model assumes a moment μ_n for an Fe atom having n Ni nearest neighbors

of

$$\mu_n = (2.85 + 0.6n)\mu_B. \quad (1)$$

This moment determines the paramagnetic behavior of the cluster as a function of applied field H_0 and temperature. The Fe magnetic hyperfine fields at saturation, H_{sat}^n , are also assumed to be functions of n . The distribution in the population of n is taken to be that appropriate to a random alloy of the concentration in question. Models of this type are not new. What is unique here is that this particularly simple model, effectively with one adjustable parameter,¹² predicts both the splitting and the complex shapes¹³ of spectra for a variety of fields, temperatures, and alloy compositions, as seen in Fig. 1. (The induced and applied fields are opposed, hence the net average hyperfine field can, and does, go through a minimum. Note the ability to predict the temperatures at which these minima occur.) While satisfactory, the agreement between the model and experiment is inferior to that often obtained in parametrized fits of Mössbauer spectra. Fits of similar quality could be made here by the explicit inclusion of additional adjustable parameters, attributed to more-distant-neighbor or other effects. Such will not be done here. As is true with almost all such fits, the fitting would not be unique and the "improvements" would be within the noise of the model and the experiments.

The giant moment clusters of the critical re-